JOURNAL OF ENVIRONMENTAL SCIENCES XX (2016) XXX–XXX

Available online at www.sciencedirect.com

ScienceDirect

www.elsevier.com/locate/jes

JES JOURNAL OF ENVIRONMENTAL SCIENCES

www.jesc.ac.cn

# Phosphate adsorption performance of a novel filter substrate made from drinking water treatment residuals

*Wendong Wang*[1,2,*], *Cui Ma*[1], *Yinting Zhang*[1], *Shengjiong Yang*[1], *Yue Shao*[3], *Xiaochang Wang*[1]

1. *Department of Environmental and Municipal Engineering, Xi'an University of Architecture and Technology, Xi'an 710055, China. E-mail: wwd@xauat.edu.cn*
2. *Zhejiang Provincial Key Laboratory of Water Science and Technology, Zhejiang 314006, China*
3. *Department of Chemical and Biomolecular Engineering, Rice University, Houston 77005, USA*

ARTICLE INFO

*Article history:*
Received 4 December 2015
Revised 20 January 2016
Accepted 26 January 2016
Available online xxxx

*Keywords:*
Adsorption
Drinking water treatment residuals
Domestic wastewater
Filter substrate
Phosphate

ABSTRACT

Phosphate is one of the most predominant pollutants in natural waters. Laboratory experiments were conducted to investigate the phosphate adsorption performance of a (NFS) made from drinking water treatment residuals. The adsorption of phosphate on the NFS fitted well with the Freundlich isotherm and pseudo second-order kinetic models. At pH 7.0, the maximum adsorption capacity of 1.03 mg/g was achieved at 15°C corresponding to the wastewater temperature in cold months, and increased notably to 1.31 mg/g at 35°C. Under both acidic conditions (part of the adsorption sites was consumed) and basic conditions (negative charges formed on the surface of NFS, which led to a static repulsion of $PO_4^{3-}$ and $HPO_4^{2-}$), the adsorption of phosphate was slightly inhibited. Further study showed that part of the adsorption sites could be recovered by 0.25 mol/L NaOH. The activation energy was calculated to be above 8.0 kJ/mol, indicating that the adsorption of phosphate on NFS was probably a chemical process. Considering the strong phosphate adsorption capacity and recoverability, NFS showed great promise on enhancing phosphate removal from the secondary treated wastewater in the filtration process.



## Introduction

Phosphate is one of the critical pollutants in natural waters (Fulazzaky et al., 2014). It is mainly produced as the result of human activities, and ultimately enters water bodies. The existence of phosphate will change the trophic state of natural waters and lead to algal bloom (Muscutt and Withers, 1996; Yang et al., 2013), which adversely affect the water quality in terms of esthetic problems (Ragheb, 2013), changing oxygen content, and thus, leading to the death of aquatic livings (Biswas et al., 2007). Besides, toxins are produced as the growth of algae. These toxins can transfer into the human body through the food chain (Yuan et al., 2006). Thus, the content of phosphate in the water environment must be controlled to maintain the ecological balance of the natural system (Conley et al., 2009).

To enhance the removal of phosphate from the wastewater, lots of methods have been developed (Hui et al., 2014; Vaiopoulou et al., 2007). Biological treatment is the most commonly used method and shows an advantage of low cost. However, the removal rate of phosphate is not stable (Vaiopoulou et al., 2007). Accordingly, chemical treatment

* *Corresponding author.*
E-mail address: wwd@xauat.edu.cn (W. Wang).

http://dx.doi.org/10.1016/j.jes.2016.01.010
1001-0742/

methods such as the addition of calcium or magnesium salts are used to guarantee phosphate removal. However, the costs of the chemical reagents are usually high, and the treatment and disposal of the chemical sludge should be considered. Besides chemical precipitation, adsorption is used to remove phosphate because of its high efficiency and easy operation (Bhattacharyya and Gupta, 2008; Palanisamy and Sivakumar, 2009; Wajima and Rakovan, 2013). Materials such as activated carbon (Zhang et al., 2011), natural clays (Mangwandi et al., 2014; Wei et al., 2014), modified clays (Yang et al., 2014; Zamparas et al., 2012), and industrial wastes (Barca et al., 2012; Rhue and Harris, 1999) have been used for phosphate removal to guarantee an advanced treated water quality.

Drinking water treatment residuals (WTR) are produced globally as a by-product of the coagulation process. Major components of WTR are soils, organic materials, and metal hydroxides/oxides, depending on the metal salt used for coagulation (Babatunde and Zhao, 2007). For the residuals produced in the plants using aluminum-based coagulants, Al is the major metal component with a weight ratio of 12% ± 2% (Ippolito et al., 2011). Other elements, such as Fe, Ca, Mg, Cr, Cu, Cd, Ni, Pb, and Zn were also detected but with a much lower weight ratio. These wastes are usually disposed off to landfills (Makris and O'Connor, 2007; Nair and Ahammed, 2015). Recently, efforts have been made to reuse WTR in water and wastewater treatments (Guan et al., 2005). Gibbons et al. (2009) studied the reuse of WTR as a coagulant for phosphate removal. It was proved to be a cost-effective adsorption material for treating wastewaters with high phosphate contents (Babatunde et al., 2011; Gao et al., 2013). However, the use of WTR as a potential filter substrate to achieve an enhanced phosphate removal has not yet been reported.

In this study, WTR were used as the major material in the production of a novel filter substrate (NFS). The aim of this work is to investigate the phosphate adsorption performances of the NFS and the possibility of utilizing the NFS as a filter substrate for the enhanced removal of phosphate from secondary treated wastewaters.

## 1. Experimental materials and methods

### 1.1. Preparation of filter substrate

The NFS used in this study was prepared from the WTR produced by a local plant in Xi'an, China. The plant is fed by the Heihe Reservoir with a total water supply capacity of 450,000 $m^3$/day. The average pH, turbidity, and total organic carbon (TOC) in the raw water was 7.6, 23.8 NTU, and 5.4 mg/L, respectively. Poly-aluminum chloride (PACl) is used as the coagulant, and the flocs formed in coagulation were the major material of NFS. Besides WTR, kaolin and humic acid were also introduced. Kaolin after calcining shows a great pozzolanic property that can enhance the strength of materials (Sabir et al., 2001). Humic acid, with a linear aggregation structure under basic conditions (He et al., 2008), will be oxidized into $CO_2$ and $H_2O$ after calcining and produce quantities of micro-pore structures, which helps to improve the specific surface area of NFS. Based on the target density ($2.1 \times 10^3$–$2.3 \times 10^3$ kg/$m^3$) and specific area of the NFS, the weight ratio of WTR:kaolin:humic acid was optimized. The preparation process was as follows: (1) drying the sludge to a constant weight at 105°C, (2) mixing the sludge trituration with kaolin and humic acid (Aldrich Chemical Company, USA) in a weight ratio of 10:7:2, (3) adding certain amount of deionized water to maintain a water ratio of 60%–65%, (4) NFS with equivalent diameters of 2–4 mm were made by heating the sludge balls at 200°C for 1.0 hr, and then 650°C for 2.0 hr.

### 1.2. Effects of pH and temperature on the adsorption of phosphate

Adsorption tests were conducted to investigate the effects of pH (at 25°C) and temperature (at pH 7.0) on the removal of phosphate, respectively. Solutions of 2.0 mg/L phosphate (50 mL) were added to test bottles with 0.5 g of NFS. HCl and NaOH solutions (0.2 mol/L) were used to adjust the pH of the adsorption system. The concentration of phosphate residual in the solution was determined after 24 hr of adsorption. Meanwhile, the speciation and solubility of phosphate in solutions with Al(III) co-existing were calculated using the VISUAL MINTEQ software (KTH Royal Institute of Technology, Sweden). All the input parameters including suspension pH, water temperature, NFS dosage, and salt contents were the same as that controlled in the adsorption tests.

### 1.3. Adsorption isotherm experiments

NFS weighing 0.5 g was added into 50 mL test bottles. Phosphate solutions were prepared with $Na_3PO_4$ and then transferred into the test bottles. The adsorption isotherm was measured with initial phosphate concentrations ranging from 1.0 to 10.0 mg/L at pH 7.0. The test bottles were placed in water bath for 24 hr at a constant temperature. Blank solution without NFS was also included. After achieving equilibrium, 10 mL water samples were taken and pretreated with a 0.45 μm filtration membrane prior to analysis. All of the experiments were conducted three times. The adsorption capacity of NFS for phosphate $q_e$ (mg/g) was calculated as described in Eq. (1):

$$q_e = \frac{(C_i - C_e) \times V}{m} \quad (1)$$

where, $C_i$ (mg/L) and $C_e$ (mg/L) are the concentrations of phosphate at initial time and when the adsorption system reached equilibrium, respectively; $V$ (mL) is the total volume of the test solution, $m$ (g) is the mass of the NFS added to the test solution, respectively. Langmuir and Freundlich models, as described in Eqs. (2) and (3) respectively (Xiong et al., 2008), were used to describe the adsorption performances of NFS for phosphate.

$$\frac{C_e}{q_e} = \frac{1}{k_a q_m} + \frac{C_e}{q_m} \quad (2)$$

$$\log q_e = \log K_f + \frac{1}{n} \log C_e \quad (3)$$

where, $q_m$ (mg/g) is the maximum adsorption capacity of the NFS; $k_a$, (L/mg) is adsorption constant, $K_f$ (mg/L) is the Freundlich constant, and $n$ (dimensionless) is the Freundlich exponent.

Please cite this article as: Wang, W., et al., Phosphate adsorption performance of a novel filter substrate made from drinking water treatment residuals, J. Environ. Sci. (2016), http://dx.doi.org/10.1016/j.jes.2016.01.010

### 1.4. Kinetic experiments

Kinetic experiments were investigated by adding 0.5 g NFS into a series of 50 mL test bottles with 5.0 mg/L phosphate solutions at 25°C. The initial pH was maintained at 7.0. Water samples were taken and analyzed after 5, 10, 30, 60, 120, 240, 480, 780, and 1440 min of adsorption. Both the pseudo first-order and pseudo second-order kinetic models were used to simulate the amount of phosphate residual at a certain adsorption time $t$ (Yang and Al-Duri, 2005).

The pseudo first-order kinetic model is shown in Eq. (4). After integration, it can be transferred into Eq. (5):

$$\frac{dq_t}{dt} = k_1(q_e - q_t) \tag{4}$$

$$\ln(q_e - q_t) = \ln q_e - k_1 t \tag{5}$$

where, $q_t$ (mg/g) and $k_1$ (1/min) are the mass of phosphate removed by per gram of NFS at time $t$ (min) and the adsorption rate constant, respectively.

The pseudo second-order model is shown in Eq. (6):

$$\frac{dq_t}{dt} = k_2(q_e - q_t)^2. \tag{6}$$

After integration, above equation can be transferred into Eq. (7):

$$\frac{t}{q_t} = \frac{1}{k_2 q_e^2} + \frac{t}{q_e} \tag{7}$$

where, $k_2$ (g/(mg·min)) is the reaction rate constant. By plotting $t/q_t$ against $t$, a linear test plot was obtained if the adsorption process fitted well with the pseudo-second-order model.

### 1.5. Desorption studies

To investigate the recovery capacity of the used NFS, 0.5 g of fresh NFS was put into test tubes with 50 mL of 5.0 mg/L phosphate solution at 25°C at pH 7.0. Waters were sampled and the residual concentrations of phosphate were analyzed after 24 hr of adsorption. Then, the used NFS was recovered with 50 mL of 0.25 mol/L NaOH for 2.0 hr. Meanwhile, the concentration of phosphate in the eluent was measured to calculate the desorbed phosphate after restoration. Then, the recovered NFS was reused in the next adsorption–regeneration cycle.

### 1.6. Water quality analysis and NFS characterization

The concentrations of calcium, magnesium, ferric, sodium, and phosphate were analyzed using an inductively coupled plasma atomic emission spectroscopy (ICP-AES) (IRIS intrepid-II, Thermo Scientific, USA). Water samples were digested with $HNO_3$ for 12 hr. The concentration of organic matters was measured by a TOC analyzer (TOC-VCPH, Shimadzu, Japan). The concentrations of $SO_4^{2-}$, $NO_3^-$, and $Cl^-$ in the adsorption system were measured by an ion chromatograph (Metrohm 761, Metrohm Ltd., Switzerland) equipped with a METROSEP anion dual 2 separator column and a conductivity detector. The flow rate of the mobile phase (a solution of 1.8 mmol/L $Na_2CO_3$ and 1.7 mmol/L $NaHCO_3$) was maintained at 1.0 mL/min. Samples were filtered using a 0.22 μm membrane and pretreated with a C18 guard column prior to analysis. The concentration of $HCO_3^-$ was determined using the standard method of GB9736-88 for the examination of water and wastewater with methyl purple as the indicator. The pH of the adsorption system was determined using a pH meter (Model 828, Thermo Electron Corporation, USA). Static leaching tests were performed to determine the leaching behaviors of aluminum and heavy metal elements in aqueous solution at pH 5.0–9.0. The tests were carried out with 0.5 g NFS in 50 mL deionized water in sealed plastic containers over 24 hr. Samples were filtered using a 0.45 μm membrane filter prior to dilution and acidification (with $HNO_3$ for 12 hr) for inductively coupled plasma mass spectrometry (ICP-MS) analysis (series 200-ElanDRC-e, PerkinElmer, USA).

The surface structure and elemental composition of NFS were examined by scanning electron microscopy (SEM) combined with an energy dispersive spectrometer (EDS) (JSM-6490LV, JEOL Ltd., Japan). Samples were sputter-coated with gold before conducting surface scanning. $N_2$ adsorption–desorption tests were carried out at 77.35 K to determine the specific surface area using a surface area analyzer (Nova 4200e, Quantachrome Instruments Corp., USA). The $pH_{pzc}$ at which zero surface charge was achieved on the NFS was determined according to the following procedure: (1) adding 0.5 g of NFS into a series of test bottles with 50 mL of deionized water, (2) adjusting the pH of the suspensions to 2.0–11.0 using 0.2 mol/L HCl or 0.2 mol/L NaOH, (3) recording the pH ($pH_i$) of the suspensions after 72 hr of slight stirring, then (4) adding 0.5 mL 2.0 mol/L NaCl to each test bottle, and recording the equilibrated pH ($pH_e$) again after 3 hr. The $pH_{pzc}$ could be obtained from the ($pH_e$–$pH_i$) *vs.* $pH_i$ plot (Uehara and Gillman, 1980).

The concentration of –OH on the surface of NFS was determined according to the method described by Van Raij and Peech (1972). Specifically, 0.5 g of the NFS was mixed with 50.0 mL of 0.01 mol/L NaCl solution and shook for 1.0 hr. The suspensions were then placed in $N_2$ protected reactors and stirred to prevent settling. Titration was carried out by adding 0.5 mol/L HCl stepwise from 0 to 13.2 mL at an increment of 0.02 mL using Metrohm 665 Dosimat titrator. Between each acid addition, 2.0 min were allowed for pH equilibration. The pH after equilibration of each step of titration was recorded. Based on the volume corresponding to a total proton monolayer coverage ($V_e$) which was calculated from pH *vs.* $V_t$ (volume of acid added) plot, the concentration of –OH sites could be calculated (Sajidu et al., 2006).

## 2. Results and discussion

### 2.1. Effects of initial concentration on the adsorption of phosphate

The average removal rate of phosphate was approximately 80% at 25°C, which was greater at lower initial phosphate concentrations and continuously decreased as the initial concentration of phosphate increased (Fig. 1a). The highest removal rate of 84% was achieved at an initial concentration of 2.0 mg/L. Meanwhile, a tendency for adsorption capacity increases with the increase of

Please cite this article as: Wang, W., et al., Phosphate adsorption performance of a novel filter substrate made from drinking water treatment residuals, J. Environ. Sci. (2016), http://dx.doi.org/10.1016/j.jes.2016.01.010

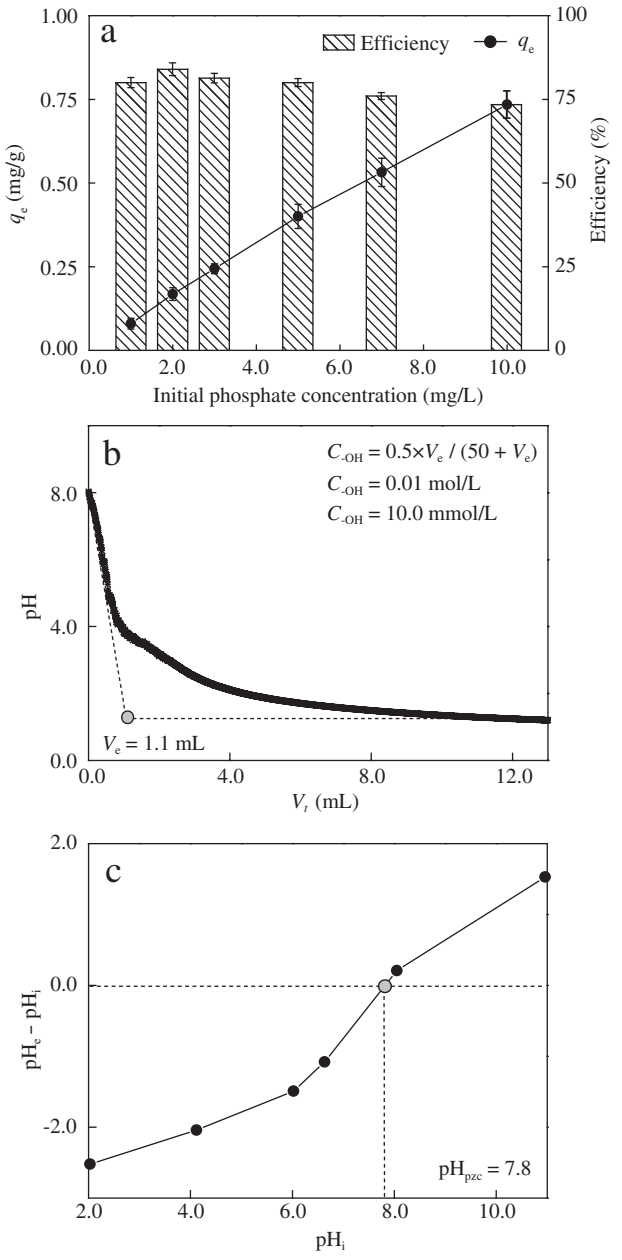


**Fig. 1 – Effect of initial contents on the adsorption of phosphate at pH 7.0 and 25°C (a), and the curves used to determine the concentration of surface –OH (b) and $pH_{pzc}$ of the novel filter substrate (NFS) (c). Error bars represent standard error of 3 replicates.**

initial concentration was observed. This tendency could be explained by the following reasons: (1) higher initial concentration supplied more adsorbates, and (2) higher initial concentration led to a sharper concentration gradient between the inner and outer sides of the interface, hence, a stronger driving force on the mass transfer of phosphate from aqueous to adsorbent. Thus, a higher initial phosphate concentration enhanced the adsorption capacity of NFS but reduced the removal efficiency of phosphate.

The NFS used in our study showed a porous structure (Appendix A Fig. S1a). The results of the BET analysis indicated a specific surface area of 72.52 $m^2/g$ for the NFS, which was much higher than that of similar materials, such as slag (1.11 $m^2/g$) and red mud (14.09 $m^2/g$) (Yang et al., 2013). The large specific area enables the NFS providing more available adsorption sites, such as –OH on the surface of NFS. From the equilibrium volume ($V_e$) shown in Fig. 1b, the concentration of adsorption sites (–OH) was calculated to be 10.0 mmol/L, much higher than that of generally used inorganic adsorbents, such as the modified clay (0.51 mmol/L) (Sajidu et al., 2006). After adsorption, however, the porous structure of the NFS diminished (Appendix A Fig. S1b), which might be related to the sedimentation of phosphate and blocked parts of the micro-channels.

### 2.2. Effects of initial pH on the adsorption of phosphate

Based on the speciation and solubility curves of phosphate, which were drawn with the data obtained using the VISUAL MINTEQ software calculation, it was concluded that the dominant phosphate species varies with the changing of pH (Fig. 2a). Fig. 2b details the residual phosphate concentration in equilibrium at 25°C, which decreased with the increase of pH under acidic conditions. The optimum removal efficiency was achieved at a pH of 7.0. On the contrary, the residual phosphate concentration in equilibrium increased with the continuous increase of pH under basic conditions. This finding was similar to the conclusion made by Yang et al. (2013) that the adsorption capacity decreased with either decreasing or increasing pH using Kanuma mud as a phosphate absorbent. However, the maximum phosphate adsorption occurred at pH 6.0 in their study, not under neutral conditions. This difference might be related to the chemical composition and the surface properties of the adsorbents, which would be explained in detail in the following discussion.

EDS analysis results showed that the major elemental composition of the NFS were O, Si, Al, Fe, Mg, and Ca, with a weight ratio of 57.15%, 20.33%, 19.52%, 1.26%, 0.49%, and 0.38%, respectively. Other elements including Cr, Cu, Cd, Ni, Pb, and Zn only occupied 0.87%, and the quantities of them leaching into the adsorption system could be ignored (Appendix A Table S1). Considering that NFS was made from drinking water treatment residuals, aluminum oxides/hydroxides and kaolin were the major components. Besides aluminum hydroxides, metal oxides on the surface of NFS could also provide –OH through the hydrolytic process as shown in Reaction (8). Quantities of –OH existing on the water–solid interface enabled NFS showing a strong reaction activity.

$$\equiv M_xO_y + yH_2O \rightarrow \equiv M_x(OH)_{2y} \quad (8)$$

where, M stands for the metal elements, such as Al(III) existing on the surface of NFS. Considering the protonation of –OH and phosphate speciation under different pH conditions (Fig. 2a), Reactions (9)–(11) might be included in the adsorption of phosphate on NFS:

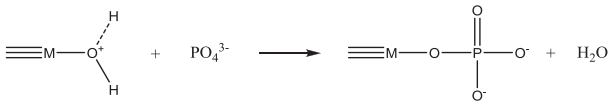

(9)

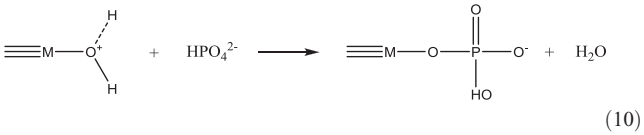

(10)

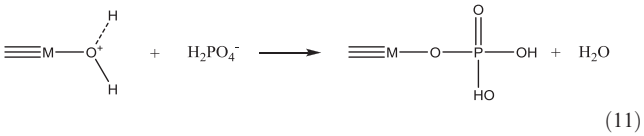

(11)

The phosphate adsorption capacity of NFS was comparatively low at pH 2.0–5.0 (Fig. 2b). One explanation is that the quantities of $H^+$ became larger under acidic conditions. This resulted in $OH^-$ being consumed and hence part of the adsorption sites destructed. Furthermore, phosphate mainly exists in the form of $H_3PO_4$ and $H_2PO_4^-$ at pH 2.0–5.0 (Fig. 2a). $H_2PO_4^-$ could be well adsorbed by the NFS, but $H_3PO_4$ shows limited adsorption because of its stable structure, resulting in a decrease in adsorption capacity. At pH 5.0–8.0, the dominant phosphate species were $H_2PO_4^-$ and $HPO_4^{2-}$, which supported the findings that $H_2PO_4^-$ and $HPO_4^{2-}$ were well adsorbed by the NFS (Fig. 2b). Meanwhile, the largest amount of Al(III) leaching out of the NFS was determined to be 0.015 mg/g in 24 hr, corresponding to 0.15 mg/L of Al(III) in the adsorption system (Appendix A Table S1). Based on thermodynamic calculation results using the VISUAL MINTEQ software, the concentrations of soluble phosphate equilibrated with $AlPO_4$(s) were all above 1.5 mg/L (Fig. 2a), much higher than that determined under the same conditions (Fig. 1a). This indicated that the contribution of chemical precipitation to the removal of phosphate could be ignored.

The $pH_{zpc}$ of the NFS was determined to be 7.8 (Fig. 1c). Accordingly, at pH values above 8.0, the surface of the adsorbent showed a negative charge, which led to a static repulsion of $PO_4^{3-}$ and $HPO_4^{2-}$, and thus, inhibited the removal of phosphate through adsorption. Meanwhile, the concentration of $OH^-$ which might form competitive adsorption with phosphate increased with the increase of pH (Yang et al., 2006).

It should be noted that the equilibrium pH of the adsorption system was stable (7.0–7.5) when the initial pH ranged from 5.0 to 10.0, indicating a potential of this adsorbent adjusting the solution pH (Fig. 2b). At pH below 7.0, metal oxidations in the NFS were hydrolyzed and released quantities of $OH^-$. The released $OH^-$ might potentially consume part of the $H^+$ as described in Reaction (12). On the contrary, when the solution pH was above 7.0, the de-protonation of metal oxides and hydroxides might occur, which resulted in a release of $H^+$ as described in Reaction (13). The released $H^+$ could react with $OH^-$. Similar reactions also occurred for the metallic hydrolytic products that existed in the NFS, as described in Reactions (13) and (14). This release of $H^+$ and $OH^-$ suggested that the above mechanism was responsible for stabilizing the pH as supported by the experimental results.

$$\equiv M_xO_y + yH_2O = xM^{2y/x} + 2yOH^- \quad (12)$$

$$\equiv M_x(OH)_{2y} = \equiv M_xO_{2y} + 2yH^+ \quad (13)$$

$$\equiv M_x(OH)_{2y} = xM^{2y/x} + 2yOH^-. \quad (14)$$

### 2.3. Kinetics

During the initial 4 hr, phosphate was rapidly adsorbed, and then the uptake rate decreased sharply (Fig. 3a). The faster uptake stage of the NFS was much shorter than that of gravels and red mud, achieved in 12 hr and 6 hr, respectively (Mann and Bavor, 1993; Mohanty et al., 2004). Meanwhile, the adsorption capacity of the NFS was 0.48 mg/g. This indicated that NFS is a competitive adsorbent for phosphate removal. The contents of both phosphate ions and available vacant adsorption sites were magnanimous at the beginning of adsorption, corresponding to a rapid phosphate and adsorption site binding rate. As the adsorption went on, the available

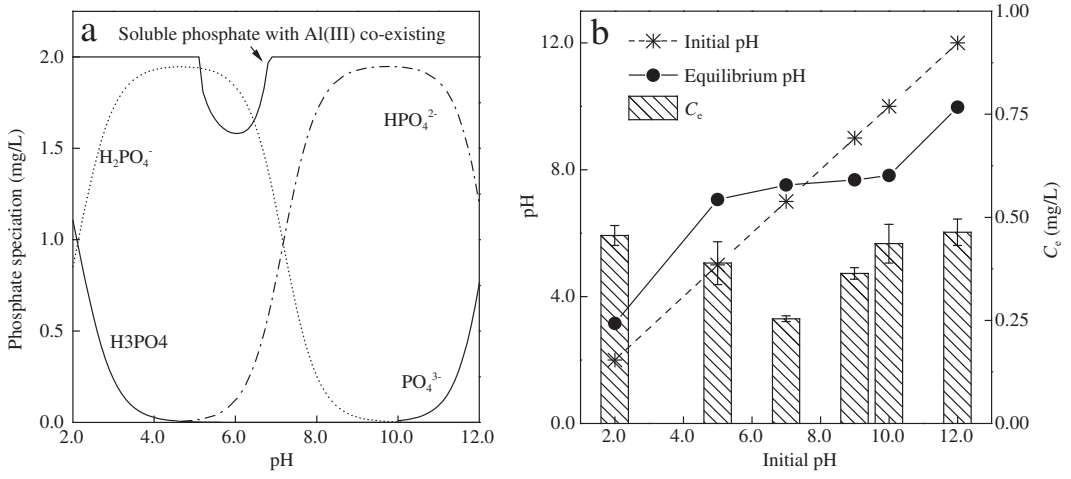


**Fig. 2 – Effects of pH on phosphate distribution and soluble phosphate concentration with 0.15 mg/L Al(III) co-existing (a), and the residual concentration of phosphate in the system with 0.5 g NFS addition (b) at 25°C (initial phosphate = 2.0 mg/L). Error bars represent standard error of 3 replicates.**

Please cite this article as: Wang, W., et al., Phosphate adsorption performance of a novel filter substrate made from drinking water treatment residuals, J. Environ. Sci. (2016), http://dx.doi.org/10.1016/j.jes.2016.01.010

adsorption sites and phosphate ions in solution were both reduced. Thus, the removing rate phosphate decreased.

Plots of different kinetic models applied are given in Fig. 3b. The adsorption kinetic behavior of NFS for phosphate ion was well described by the pseudo second-order kinetic model as its $R^2$ value was close to unity (Fig. 3b). The reaction rate constant ($k_2$) was calculated to be 0.050 g/(mg·min). Conversely, desorption could be used to recover the adsorption capacity of the NFS and being reused. In this study, 0.25 mol/L of NaOH was used as an eluent. The recovered NFS was repeatedly used for phosphate removal (Fig. 4). Overall, the phosphate removal rate decreased from 80.0% to 31.4% after 4 adsorb–desorb cycles, indicating an adsorption capacity loss and part of the adsorption sites are not recoverable. In second and third adsorb–desorb cycles, the amount of adsorbed phosphate was much higher than that desorbed in the previous cycle. This indicated that vacant adsorption sites still existed even after the adsorption process in the second adsorb–desorb cycle. In the fourth adsorb–desorb cycle, however, because most of the vacant adsorption sites had been consumed, the phosphate was mainly adsorbed by the recoverable adsorption sites, and thus led to a low adsorption but high recovery efficiency.

## 2.4. Isotherms and thermodynamics

### 2.4.1. Adsorption isotherm

The adsorption process of phosphate on the NFS fitted both the Langmuir and Freundlich models well, with correlation coefficients greater than 0.98 (Fig. 5). This finding was similar to that obtained using soils, slags and zeolite as adsorbents (Sakadevan and Bacor, 1998). As shown in Fig. 5a, the amount of phosphate adsorbed by NFS increased with water temperature. The maximum adsorption capacity ($q_m$) was calculated by plotting $C_e$ against $C_e/q_e$. In this study, the value of $q_m$ was 1.03 mg/g at 15°C, corresponding to the wastewater temperature in cold months, and increased to 1.21 and 1.33 mg/g at 25°C and 35°C, respectively, corresponding to the wastewater temperature in hot months (Fig. 5b). $k_a$ in Langmuir model exhibited an equal ratio of the desorption and adsorption rates. In this study, the $k_a$ value increased gradually as the increase of water temperature, indicating an easier executed adsorption at higher temperatures. Meanwhile, the values of $n$ obtained at 15°C, 25°C, and 35°C were all above 1.0 (Fig. 5c), indicating that NFS was effective for phosphate adsorption (Ng et al., 2002).

### 2.4.2. Thermodynamics

The relationships between Gibbs free energies ($\Delta G$), enthalpy ($\Delta H$), entropy ($\Delta S$) and distribution coefficient were shown in Eqs. (15)–(17) (El-Shahawi and Nassif, 2003):

$$K_D = \frac{C_0 - C_t}{C_t} \times \frac{V}{m} \tag{15}$$

$$\ln(K_D) = \frac{-\Delta H}{R \cdot T} + \frac{\Delta S}{R} \tag{16}$$

$$\Delta G = \Delta H - T \cdot \Delta S \tag{17}$$

where, $C_0$ (mg/L) and $C_t$ (mg/L) are the concentrations of phosphate at initial time and time $t$, respectively; $V$ (mL) is the total volume of the test solution; and $m$ (g) is the dosage of the NFS.

Thermodynamics parameters of the adsorption process of phosphate on NFS was computed by plotting $\ln(q_e/C_e)$ versus $q_e$. $\Delta H$ and $\Delta S$ could be obtained by plotting $\ln K_D$ versus $1/T$ using Eqs. (15) and (16). $R$ equals 8.314 J/(mol·K). $T$ (K) is the absolute temperature of the adsorption system. The change in Gibbs free energies ($\Delta G$) was calculated with Eq. (17). Findings showed that negative values for the $\Delta G$ (Table 1), indicating that the adsorption of phosphate on the NFS could be conducted spontaneously. $\Delta G$ decreased with the increase of temperature, implying a more favorable process at high temperatures. Further, a positive $\Delta H$ indicated that the adsorption behavior of NFS was an endothermic process.

The formation of surface complexes could be conceptualized similarly to what happened in solutions (Schindler, 1981). Based on the Gibbs free energy, the equilibrium constant ($K$) of

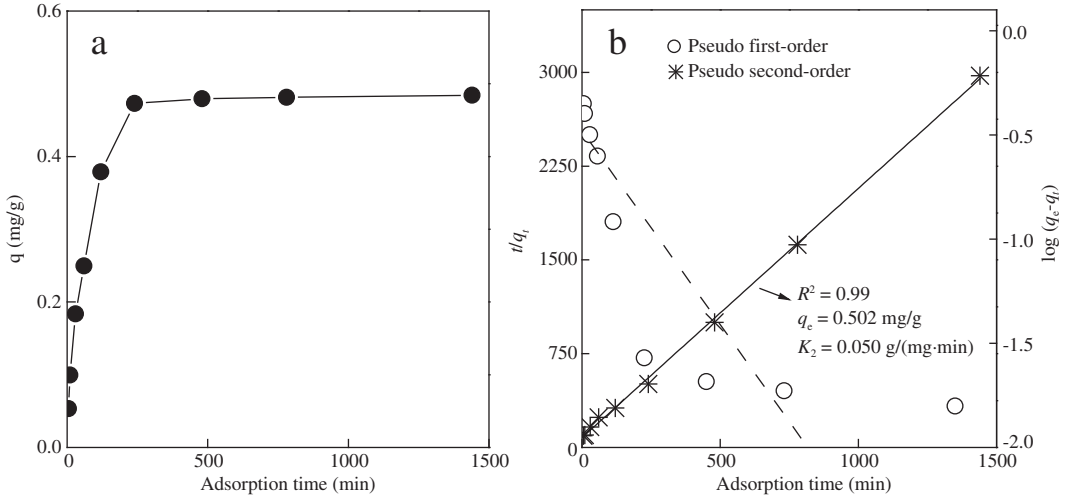


**Fig. 3 – Variation of adsorption quantity with adsorption time (a), and corresponding fitting results with pseudo-first-order and pseudo-second-order kinetic models (b) at 25°C, with an initial phosphate content and solution pH at 5.0 mg/L and 7.0, respectively.**

Please cite this article as: Wang, W., et al., Phosphate adsorption performance of a novel filter substrate made from drinking water treatment residuals, J. Environ. Sci. (2016), http://dx.doi.org/10.1016/j.jes.2016.01.010

phosphate adsorbed on the NFS was calculated with Eq. (18) to be 4.39 at 25°C. With initial phosphate and adsorption site concentrations of 0.021 and 10.0 mmol/L, respectively, the calculated equilibrium concentration of phosphate was predicted to be 0.42 mg/L applying VISUAL MINTEQ software. This value was close to the value determined under the same experimental condition (Fig. 2b). This further indicated that adsorption mainly contributed to the removal of phosphate even under neutral conditions.

$$K = \frac{-\Delta G}{RT} \tag{18}$$

### 2.4.3. Activated energy

Activated energy (E) described by Eq. (19) reveals the type of the adsorption process. The coefficient K' could be calculated by fitting $\ln(q_e)$ versus $\varepsilon^2$ as shown in Fig. 6. The slope of the fitting line was the K' value described in Eq. (20), in which $\varepsilon = RT\ln(1+\frac{1}{C_e})$.

$$E = \frac{1}{\sqrt{-2K'}} \tag{19}$$

$$\ln q_e = \ln q_m + K'\varepsilon^2 \tag{20}$$

where, E (kJ/mol) is the activated energy, K' is a constant, and $\varepsilon$ is the Polanyi energy.

Based on the value of K', the activated energy (E) could be calculated. They were 8.98, 9.53, and 9.91 kJ/mol at 15°C, 25°C, and 35°C, respectively. Because the value of E is above 8.0 kJ/mol, the adsorption of phosphate on the NFS was considered to be a chemical process (El-Shahawi and Nassif, 2003), supporting the conclusion made in Section 2.3.

## 2.5. Discussion

Compared with deionized water, the composition of wastewater was more complex. Further studies were conducted to determine the effects of co-existing materials on the adsorption of phosphate at 25°C, following the procedure described in Section 1.3. The initial phosphate concentration was 2.0 mg/L. Both secondary treated wastewater (STW, obtained from a local sewage plant, Xi'an, China) and 5 times diluted STW were used. The concentrations of $Ca^{2+}$, $Mg^{2+}$, $Fe^{3+}$, $Na^+$, $SO_4^{2-}$, $NO_3^-$, $HCO_3^-$, $Cl^-$, and organic matters (as TOC) in the STW were 28.1, 7.8, 0.1, 97.3, 36.9, 3.2, 58.8, 153.9, and 9.2 mg/L, respectively. The phosphate removal rate of the system prepared with STW was approximately 90%, which decreased slightly to 87.5% in the 5 times diluted STW system, close to that achieved in the system prepared with deionized water (Fig. 1a). This finding indicated that the co-existing materials do not inhibit the adsorption of phosphate. Xue et al. (2009) reported a similar observation that despite the wide variation in the concentrations of $Cl^-$, $NO_3^-$, $SO_4^{2-}$, from 100 to 1000 mg/L, there was no significant difference in the removal rate of phosphate by basic oxygen furnace slag adsorption.

The concentration of phosphate in the STW was usually in the range of 0.5–3.0 mg/L. Assuming 90% of the phosphate was removed from the STW, the phosphate saturation time could be calculated. Take a 6 m × 6 m × 1.6 m NFS filter for

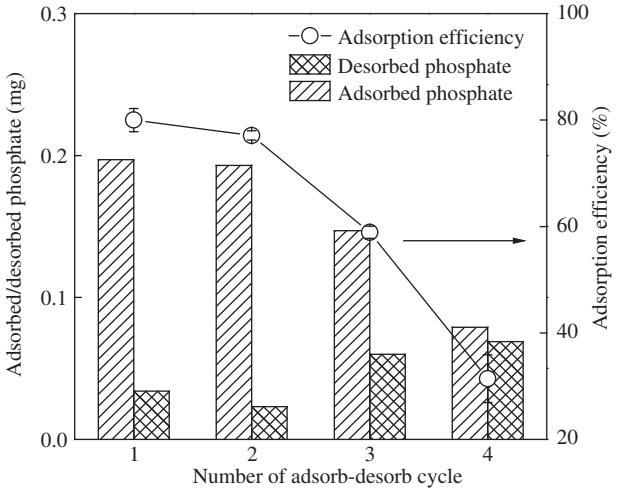


**Fig. 4 – Amounts of adsorbed/desorbed phosphate and its removal efficiency with the numbers of adsorb–desorb cycles of NFS at 25°C (pH = 7.0, initial phosphate = 5.0 mg/L). Error bars represent standard error of 3 replicates.**

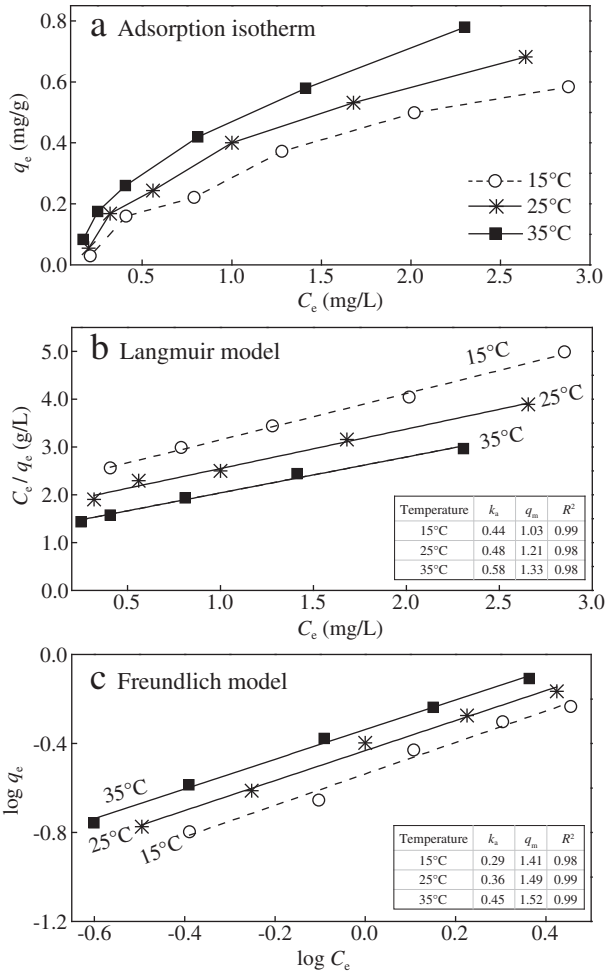


**Fig. 5 – Adsorption isotherm experimental data (a) and corresponding fitted curves based on Langmuir (b) and Freundlich (c) models, respectively (pH = 7.0, NFS dosage = 0.5 g).**

Please cite this article as: Wang, W., et al., Phosphate adsorption performance of a novel filter substrate made from drinking water treatment residuals, J. Environ. Sci. (2016), http://dx.doi.org/10.1016/j.jes.2016.01.010

**Table 1 – Thermodynamic parameters for the adsorption of $PO_4^{3-}$ on NFS.**

| ΔH (kJ/mol) | ΔS (kJ/mol) | $R^2$ | ΔG (kJ/mol) | | |
|---|---|---|---|---|---|
| | | | 288 K | 298 K | 308 K |
| 24.86 | 0.12 | 0.99 | −9.7 | −10.9 | −12.1 |

example, the maximum saturation time was in the range of 0.4–2.5 years when the system was run with an average water temperature and hydraulic loading rate at 15°C and 180 $m^3$/day, respectively. During the hot months, taking the water temperature which increased to 25°C for example, the total effectiveness of NFS would extend to 0.5–2.9 years for the STW with phosphate contents varying between 0.5 and 3.0 mg/L. Though the bench-scale experimental and calculation results could not be fully extended to pilot scale filters, the results obtained in our study provided valuable information on the adsorption and regeneration performances of the NFS and its potential use as a novel filter substrate.

## 3. Conclusions

The environmental effects of excessive phosphate have been well documented. Various treatment technologies have been explored for the enhanced removal of phosphate from wastewater. However, there are few established adsorptive filtration media that can satisfy the removal requirements for phosphate, especially the dissolved portion. In this study, a novel filter substrate (NFS) developed from drinking water treatment residuals was utilized for phosphate removal. The NFS exhibited an excellent phosphate adsorption ability compared to many other mineral adsorbents that have been recently evaluated. The data obtained from the adsorption process fitted well with both the Freundlich isotherm model and pseudo-second-order model. Under neutral conditions, a maximum adsorption capacity of 1.21 mg/g was achieved at 25°C. With the increase of temperature, the $q_m$ value increased gradually, and thus, extended the usable theoretical time of NFS. Further, the used NFS could be regenerated using NaOH as eluent. The desirable pH for phosphate adsorption was in the range of 5.0–8.0. At pH above 8.0, the adsorption of phosphate was slightly inhibited as the existence of negative charges on the surface of NFS. The results suggest that NFS filtration promises to be an effective treatment option for the enhanced removal of phosphate from the STW.

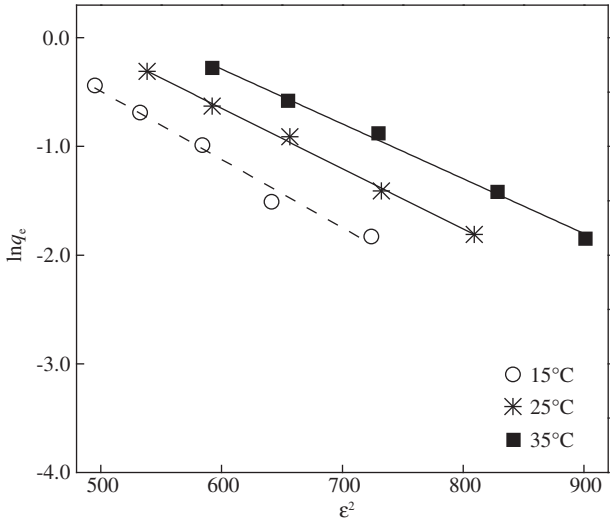


**Fig. 6 – Plots of ln($q_e$) versus $\varepsilon^2$ at 15°C, 25°C, and 35°C, respectively.**

## Acknowledgments

This research was supported by the National Natural Science Foundation of China (No. 21007050) and the Science and Technology Nova Program of Shaanxi (No. 2014KJXX-66).

## Appendix A. Supplementary data

Supplementary data to this article can be found online at http://dx.doi.org/10.1016/j.jes.2016.01.010.

## REFERENCES

Babatunde, A.O., Zhao, Y.Q., 2007. Constructive approaches toward water treatment works sludge management: an international review of beneficial reuses. Crit. Rev. Environ. Sci. Technol. 37 (2), 129–164.

Babatunde, A.O., Zhao, Y.Q., Doyle, R.J., Rackard, S.M., Kumar, J.L., Hu, Y.S., 2011. Performance evaluation and prediction for a pilot two-stage on-site constructed wetland system employing dewatered alum sludge as main substrate. Bioresour. Technol. 102 (10), 5645–5652.

Barca, C., Gérente, C., Meyer, D., Chazarenc, F., Andrès, Y., 2012. Phosphate removal from synthetic and real wastewater using steel slags produced in Europe. Water Res. 46 (7), 2376–2384.

Bhattacharyya, K.G., Gupta, S.S., 2008. Adsorption of a few heavy metals on natural and modified kaolinite and montmorillonite: a review. Adv. Colloid Interf. Sci. 140 (2), 114–131.

Biswas, B.K., Inoue, K., Ghimire, K.N., Ohta, S., Harada, H., Ohto, K., et al., 2007. The adsorption of phosphate from an aquatic environment using metal-loaded orange waste. J. Colloid Interface Sci. 312 (2), 214–223.

Conley, D.J., Paerl, H.W., Howarth, R.W., Boesch, D.F., Seitzinger, S.P., Havens, K.E., et al., 2009. Ecology: controlling eutrophication: nitrogen and phosphorus. Science 323 (5917), 1014–1015.

El-Shahawi, M.S., Nassif, H.A., 2003. Retention and thermodynamic characteristics of mercury(II) complexes onto polyurethane foams. Anal. Chim. Acta 481 (1), 29–39.

Fulazzaky, M.A., Khamidun, M.H., Din, M.F.M., Yusoff, A.R.M., 2014. Adsorption of phosphate from domestic wastewater treatment plant effluent onto the laterites in a hydrodynamic column. Chem. Eng. J. 258, 10–17.

Gao, S.J., Wang, C.H., Pei, Y.S., 2013. Comparison of different phosphate species adsorption by ferric and alum water treatment residuals. J. Environ. Sci. (China) 25 (5), 986–992.

Gibbons, M.K., Mortula, M.M., Gagnon, G.A., 2009. Phosphorus adsorption on water treatment residual solids. J. Water Supply Res Technol. 58 (1), 1–10.

Guan, X.H., Chen, G.H., Shang, C., 2005. Reuse of water treatment works sludge to enhance particulate pollutant removal from sewage. Water Res. 39 (15), 3433–3440.

He, M.C., Shi, Y.H., Lin, C.Y., 2008. Characterization of humic acids extracted from the sediments of the various rivers and lakes in China. J. Environ. Sci. (China) 20 (11), 1294–1299.

Hui, B., Zhang, Y., Ye, L., 2014. Preparation of PVA hydrogel beads and adsorption mechanism for advanced phosphate removal. Chem. Eng. J. 235, 207–214.

Ippolito, J.A., Barbarick, K.A., Elliott, H.A., 2011. Drinking water treatment residuals: a review of recent uses. J. Environ. Qual. 40, 1–12.

Makris, K.C., O'Connor, G.A., 2007. Beneficial utilization of drinking-water treatment residuals as contaminant-mitigating agents. Develop. Environ. Sci. 5, 607–636.

Mangwandi, C., Albadarin, A.B., Glocheux, Y., Walker, G.M., 2014. Removal of ortho-phosphate from aqueous solution by adsorption onto dolomite. J. Environ. Chem. Eng. 2, 1123–1130.

Mann, R.A., Bavor, H.J., 1993. Phosphorus removal in constructed wetlands using gravel and industrial waste substrata. Water Sci. Technol. 27 (1), 107–113.

Mohanty, S., Pradhan, J., Das, S.N., Thakur, R.S., 2004. Removal of phosphorus from aqueous solution using alumized red mud. Int. J. Environ. Stud. 61 (6), 687–697.

Muscutt, A.D., Withers, P.J.A., 1996. The phosphorus content of rivers in England and Wales. Water Res. 30 (5), 1258–1268.

Nair, A.T., Ahammed, M.M., 2015. The reuse of water treatment sludge as a coagulant for post-treatment of UASB reactor treating urban wastewater. J. Clean. Prod. 96, 272–281.

Ng, C., Losso, J.N., Marshall, W.E., Rao, R.M., 2002. Freundlich adsorption isotherms of agricultural by-product-based powdered activated carbons in a geosmin–water system. Bioresour. Technol. 85 (2), 131–135.

Palanisamy, P.N., Sivakumar, P., 2009. Kinetic and isotherm studies of the adsorption of Acid Blue 92 using a low-cost non-conventional activated carbon. Desalination 249 (1), 388–397.

Ragheb, S.M., 2013. Phosphate removal from aqueous solution using slag and fly ash. HBRC J. 9 (3), 270–275.

Rhue, R.D., Harris, W.G., 1999. In: Reddy, K.R., O'Connor, G.A., Schelske, C.L. (Eds.), Phosphorus Sorption/Desorption Reactions in Soils and Sediments. In Phosphorus Biogeochemistry in Subtropical Ecosystems. Lewis, Boca Raton.

Sabir, B.B., Wild, S., Bai, J., 2001. Metakaolin and calcined clays as pozzolans for concrete: a review. Cem. Concr. Compos. 23, 441–454.

Sajidu, S.M.I., Persson, I., Masamba, W.R.L., Henry, E.M.T., Kayambazinthu, D., 2006. Removal of $Cd^{2+}$, $Cr^{3+}$, $Cu^{2+}$, $Hg^{2+}$, $Pb^{2+}$ and $Zn^{2+}$ cations and $AsO_4^{3-}$ anions from aqueous solutions by mixed clay from Tundulu in Malawi and characterisation of the clay. Water SA 32 (4), 519–526.

Sakadevan, K., Bacor, H.J., 1998. Phosphate adsorption characteristics of soils, slags and zeolite to be used as substrates in constructed wetland systems. Water Res. 32 (2), 393–399.

Schindler, P.W., 1981. Surface complexes at oxide–water interfaces. In: Anderson, M., Rubin, A. (Eds.), Adsorption of Inorganics at Solid–Liquid Interfaces. Ann Arbor Science, Ann Arbor, Michigan.

Uehara, G., Gillman, G.P., 1980. Charge characteristics of soils with variable and permanent charge minerals. II. Experimental. Soil Sci. Soc. Am. J. 44, 250–251.

Vaiopoulou, E., Melidis, P., Aivasidis, A., 2007. Growth of filamentous bacteria in an enhanced biological phosphorus removal system. Desalination 213, 288–296.

Van Raij, B.V., Peech, M., 1972. Electrochemical properties of some oxisols and alfisols of the tropics. Soil Sci. Soc. Am. Proc. 36, 587–593.

Wajima, T., Rakovan, J.F., 2013. Removal behavior of phosphate from aqueous solution by calcined paper sludge. Colloids Surf., A 435 (9), 132–138.

Wei, S.Y., Tan, W.F., Liu, F., Zhao, W., Weng, L.P., 2014. Surface properties and phosphate adsorption of binary systems containing goethite and kaolinite geoderma. Environ. Sci. 213, 478–484.

Xiong, J., He, Z., Mahmood, Q., Liu, D., Yang, X., Islam, X., 2008. Phosphate removal from solution using steel slag through magnetic separation. J. Hazard. Mater. 152 (1), 211–215.

Xue, Y.J., Hou, H.B., Zhu, S.J., 2009. Characteristics and mechanisms of phosphate adsorption onto basic oxygen furnace slag. J. Hazard. Mater. 162, 973–980.

Yang, X., Al-Duri, B., 2005. Kinetic modeling of liquid-phase adsorption of reactive dyes on activated carbon. J. Colloid Interface Sci. 287 (1), 25–34.

Yang, Y., Zhao, Y.Q., Babatunde, A.O., Wang, L., Ren, Y.X., Han, Y., 2006. Characteristics and mechanisms of phosphate adsorption on dewatered alum sludge. Sep. Purif. Technol. 51 (2), 193–200.

Yang, S.J., Ding, D.H., Zhao, Y.X., Huang, W.L., Zhang, Z.Y., Lei, Z.F., et al., 2013. Investigation of phosphate adsorption from aqueous solution using Kanuma mud: behaviors and mechanisms. J. Environ. Chem. Eng. 1, 355–362.

Yang, M.J., Lin, J.W., Zhan, Y.H., Zhang, H.H., 2014. Adsorption of phosphate from water on lake sediments amended with zirconium-modified zeolites in batch mode. Ecol. Eng. 71, 223–233.

Yuan, M., Carmichael, W.W., Hilborn, E.D., 2006. Microcystin analysis in human sera and liver from human fatalities in Caruaru. Toxicon 48 (6), 627–640.

Zamparas, M., Gianni, A., Stathi, P., Deligiannakis, Y., Zacharias, I., 2012. Removal of phosphate from natural waters using innovative modified bentonites. Appl. Clay Sci. 62-63, 101–106.

Zhang, L., Wan, L.H., Chang, N., Liu, J.Y., Duan, C., Zhou, Q., et al., 2011. Removal of phosphate from water by activated carbon fiber loaded with lanthanum oxide. J. Hazard. Mater. 190 (1–3), 848–855.

Please cite this article as: Wang, W., et al., Phosphate adsorption performance of a novel filter substrate made from drinking water treatment residuals, J. Environ. Sci. (2016), http://dx.doi.org/10.1016/j.jes.2016.01.010